Zhengjin Wang
State Key Laboratory for Strength and
Vibration of Mechanical Structures,
International Center for Applied Mechanics,
School of Aerospace Engineering,
Xi'an Jiaotong University,
Xi'an 710049, China;
School of Engineering and Applied Sciences,
Kavli Institute for Nanobio Science and
Technology,
Harvard University,
Cambridge, MA 02138

Yucun Lou
Schlumberger-Doll Research,
One Hampshire Street,
Cambridge, MA 02139

Zhigang Suo
School of Engineering and Applied Sciences,
Kavli Institute for Nanobio
Science and Technology,
Harvard University,
Cambridge, MA 02138
e-mail: suo@seas.harvard.edu

Crack Tunneling in Cement Sheath of Hydrocarbon Well

In a hydrocarbon well, cement fills the annular gap between two steel casings or between a steel casing and rock formation, forming a sheath that isolates fluids in different zones of the well. For a well as long as several kilometers, the cement sheath covers a large area and inevitably contains small cracks. The cement sheath fails when a small crack grows and tunnels through the length of the well. We calculate the energy release rate at a steady-state tunneling front as a function of the width of the tunnel. So long as the maximum energy release rate is below the fracture energy of the cement, tunnels of any width will not form. This failsafe condition requires no measurement of small cracks, but depends on material properties and loading conditions. We further show that the critical load for tunneling reduces significantly if the cement/casing and cement/formation interfaces slide. [DOI: 10.1115/1.4031649]

Keywords: wellbore cement, crack tunneling, friction

Introduction

Horizontal drilling and hydraulic fracturing have been pushing hydrocarbon wells to produce under extreme operational conditions and rigorous environmental regulations [1–4]. Geopolitical and financial turbulence aside, these technological advances have stimulated scientific research in oilfield mechanics and materials. Examples include mechanisms of hydraulic fracture [5–7], buckling in horizontal drilling [8], rheology of hydraulic fracturing proppants [9,10], mechanics of rubber–cement composite seals [11], swelling and leak of elastomeric seals [12–16], and downhole degradable composites [17,18].

This paper focuses on the fracture mechanics of cement, a material of choice in oilfields due to its low cost, low permeability, and ability to set in water, gas, and oil. Cement is commonly used as a sheath to fill the annular gap between two steel casings or between a steel casing and rock formation. The cement sheath prevents corrosion of the steel casings, provides mechanical support and, most importantly, isolates fluids in different zones of the well throughout its lifetime [19]. Even if the cement is initially properly set, it may damage due to, e.g., the drilling of wellbore, perforation of casing, and hydraulic stimulation of reservoir [20–22]. A damaged cement sheath may result in loss of hydrocarbon production, environmental pollution, and catastrophic disasters [23,24].

The current approach to the design of cement sheaths is through stress analysis [22,25–29]. This approach calculates the stress field using the linear theory of elasticity and obtains the critical condition for failure according to the Mohr–Coulomb or other strength criteria [22,25]. This approach is used to determine the critical external load and choose cement.

For a well as long as several kilometers, a cement sheath covers a large area and inevitably contains many small cracks, caused by, e.g., shrinkage during cement hydration, perforation, and hydraulic fracturing. So long as these small cracks remain stable, they do not impair the functions of the cement sheath. Under some conditions, however, the small cracks grow into large cracks. Growth of cracks in the radial direction of a cement sheath has been studied recently [30]. Such radial cracks cause local damage. The failure criterion developed in this approach depends on the location and size of the initial cracks, which cannot be measured in a long well.

Several experimental observations have led us to study a crack tunneling along the length of a cement sheath [29,31]. Boukhelifa et al. [32] observed that permeability of cement increased two orders of magnitude due to the crack generated by the loading cycles. We calculate the energy release rate at steady-state tunneling front. The energy release rate varies with the width of the tunnel and reaches the maximum value for a particular width of the tunnel. So long as the maximum energy release rate is below the fracture energy of the cement, tunnels of any width will not form. This condition provides a failsafe criterion that requires no measurement of the sizes of the small cracks, but depends on material properties and loading conditions. Furthermore, we show that the critical load for tunneling greatly reduces when frictional sliding of the cement/casing and cement/formation interfaces slides.

Steady-State Tunneling Crack

Consider a cement sheath, inner and outer radii R_c and R_b, filling the gap between a steel casing and rock formation (Fig. 1(*a*)). Let $t_c = R_b - R_c$ be the thickness of the cement sheath and t_s be the thickness of the steel casing. The pressure p inside the steel casing may arise from changes in the downhole conditions or wellbore operations. The internal pressure causes a field of stress, taken to be invariant along the length of the well—that is, the well is assumed to deform under the plane strain conditions. In the absence of cracks, the hoop stress in the cement sheath is usually tensile, maximizes near the casing/cement interface, and decreases

Contributed by the Applied Mechanics Division of ASME for publication in the Journal of Applied Mechanics. Manuscript received September 17, 2015; final manuscript received September 21, 2015; published online October 8, 2015. Editor: Yonggang Huang.

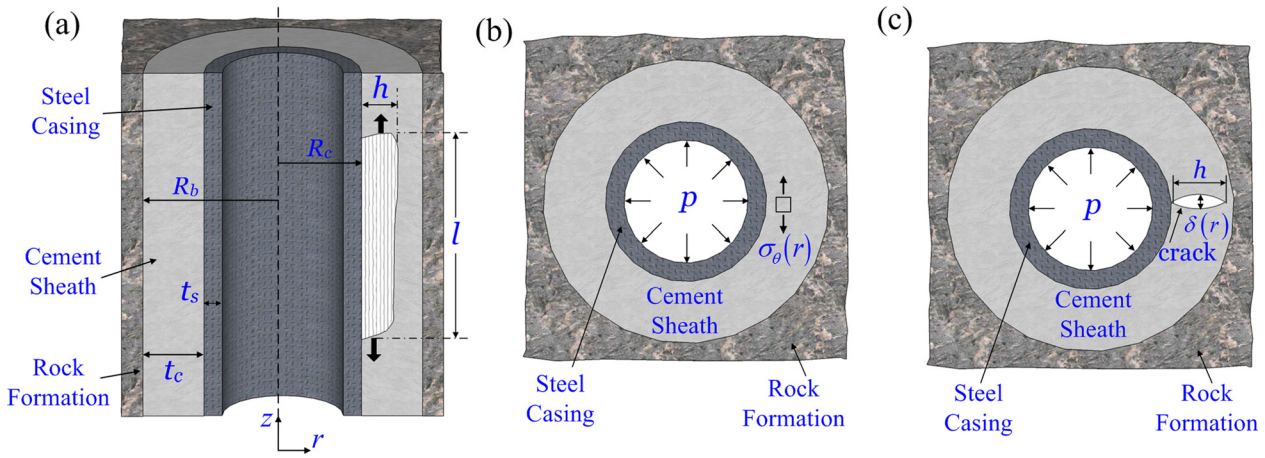

Fig. 1 A crack tunnel in a cement sheath. (*a*) A cross section along the length of a well. A cement sheath fills the gap between a steel casing and rock formation. A crack tunnel in the cement sheath. (*b*) A cross section normal to the well, far ahead the tunnel front. The pressure inside the steel casing causes a stress field in the cement sheath. (*c*) A cross section normal to the well, far behind the tunnel front. The pressure inside the steel casing causes the crack to open in the cement.

and may even become compressive as the cement/formation interface is approached [22].

A crack is confined within the cement sheath, but can tunnel along the length of the well. The crack propagating in cement is tortuous at a small scale, but creates a distinct path at a scale of the sheath, as observed in experiments [29,31]. In calculating energy release rate, we assume that the faces of the crack are flat. Let l be the length and h be the width of the tunnel. Also, the strength of cement is known to have pronounced tension–compression asymmetry. Here, we assume that the compressive strength is much larger than tensile strength and will only consider failure under tensile conditions. The energy release rate of the tunneling crack, G, is defined as the reduction of the potential energy of the system associated with the tunnel elongating along the length of the well by unit area. Everything else being fixed, the energy release rate of the tunneling crack increases with the length l. When $l/h > 2$, the tunneling crack approaches a steady state, namely, the energy release rate becomes independent of the length of the tunnel [33]. Following the linear elastic fracture mechanics, the normalized steady-state tunneling energy release rate takes the form

$$\frac{GE_f}{R_b p^2} = M\left(\frac{h}{t_c}, \frac{t_s}{t_c}, \frac{R_b}{t_c}, \frac{E_c}{E_f}, \nu_c, \frac{E_s}{E_f}, \nu_f, \nu_s \ldots\right) \tag{1}$$

where M is a dimensionless function of dimensionless groups, E and ν are the Young's modulus and Poisson's ratio, with the subscripts c, f, and s indicating the cement, formation, and steel casing, respectively.

The tunneling front advances in a three-dimensional elastic field. In the steady state, however, the energy release rate at the tunneling front can be calculated by using two fields under plane strain conditions. The first field exists far ahead the tunneling front, where $\sigma_\theta(r)$ is the hoop stress in the cement prior to the arrival of the tunneling front (Fig. 1(*b*)). The second field exists

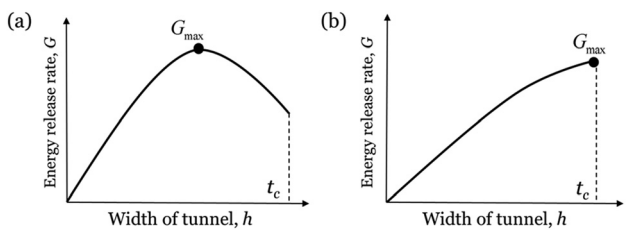

Fig. 2 The energy release rate of a steady-state tunneling crack is a function of the width of the tunnel, $G(h)$. (*a*) In some cases, the energy release rate reaches maximum G_{max} when the width of the tunnel is less than the thickness of the cement sheath. (*b*) In other cases, the energy release rate monotonically increases with the width of the tunnel.

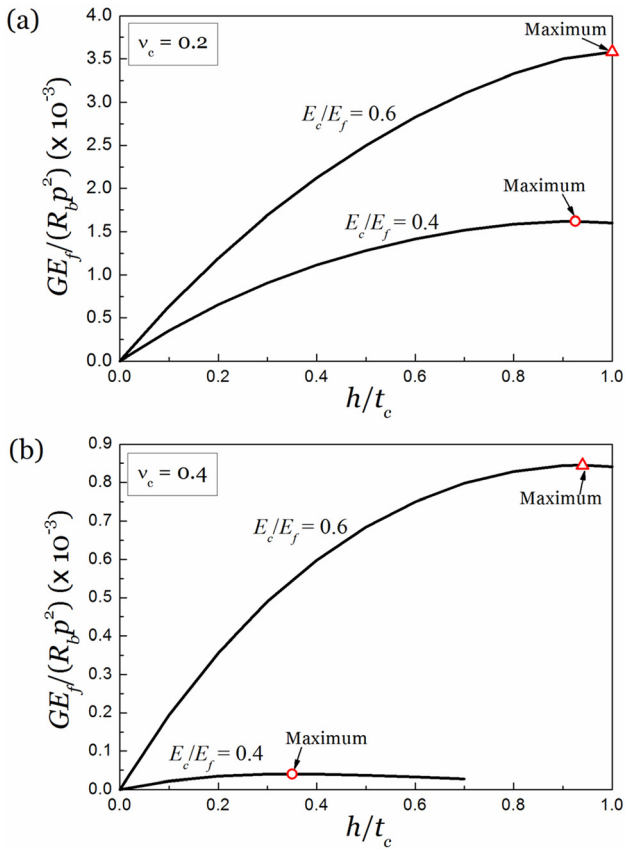

Fig. 3 The normalized energy release rate as a function of the normalized width of the tunnel: (*a*) ν_c=0.2 and (*b*) ν_c=0.4

far behind the tunneling front, where $\delta(r)$ is the opening displacement of the crack (Fig. 1(*c*)). The energy release rate at the steady-state tunneling front is given by [34]

$$G = \frac{1}{2h}\int_0^h \sigma_\theta(r)\delta(r)dr \tag{2}$$

The calculations of $\sigma_\theta(r)$ and $\delta(r)$ are discussed in Appendices A and B, respectively.

The tunneling energy release rate is a function of the width of the tunnel, $G(h)$. In some cases, the tunneling energy release rate reaches maximum when the width of the tunnel is less than the thickness of the cement sheath (Fig. 2(*a*)). In other cases, the tunneling energy release rate monotonically increases with the width of the tunnel (Fig. 2(*b*)). In either case, denote the maximum tunneling energy release rate by $G_{\max}$. Denote the fracture energy of the cement by Γ_c. Small cracks of random sizes, orientations, and locations likely exist in the cement sheath. If $G_{\max} > \Gamma_c$, it is likely that some of the small cracks will grow into tunnels. If $G_{\max} < \Gamma_c$, however, no small cracks can grow into tunnels. Consequently, the condition $G_{\max} < \Gamma_c$ provides a failsafe criterion that requires no measurement of the small cracks.

Failsafe Map

The failsafe condition, however, depends on material properties and operating conditions. Consider a representative wellbore geometry, $R_b/t_c = 5$ and $t_s/t_c = 0.5$. The elastic constants of the steel casing and rock formation are taken to be constants: $E_s = 200\,\text{GPa}$, $\nu_s = 0.27$, $E_f = 20\,\text{GPa}$, and $\nu_f = 0.2$. For the cement, two values of Poisson's ratios are considered, $\nu_c = 0.2$ and 0.4, representing, respectively, regular cements and cement–rubber composites [26,28,32]. Young's modulus of cement is chosen to be less than that of the rock formation, $0 < E_c/E_f < 1$. We plot the normalized tunneling energy release rate G as a function of the normalized width of the tunnel (Fig. 3). For the case $E_c/E_f = 0.6$ and $\nu_c = 0.2$, the tunneling energy release rate monotonically increases with h and reaches maximum when $h = t_c$. For all the other three cases, energy release rates reach maximum when the width of the tunnel is less than the thickness of the cement sheath. The energy release rates can be dramatically decreased by decreasing Young's modulus and increasing Poisson's ratio of cement. Therefore, a more compliant and more incompressible cement can better resist tunneling cracks. This theoretical conclusion is consistent with field observations [26,28,32]. This trend is understood: the tensile stress that drives the tunnels is lower for a cement of a lower Young's modulus and higher Poisson's ratio (Fig. 8).

We represent the failsafe criterion in the plane with the modulus contrast E_c/E_f as the horizontal axis and the normalized fracture energy $\Gamma_c E_f/(R_b p^2)$ as the vertical axis (Fig. 4). The condition $G_{\max} = \Gamma_c$ divides the plane into two regions: tunneling and no tunneling. Tunnels will not form if the cement has a high-normalized fracture energy and low-normalized Young's modulus. Also, a cement of a higher Poisson's ratio is more tunnel-resistant. These failsafe maps can be used to determine the upper bound of the internal pressure p with the knowledge of cement properties or choose the proper cement based on the loading conditions. Approaches to avoid tunneling cracks include decreasing Young's modulus of the cement, increasing Poisson's ratio of the cement, or increasing the dimensionless group $\Gamma_c E_f/(R_b p^2)$.

Cement with low Young's modulus and high fracture energy is ideal to resist tunneling. However, the fracture energy often increases with the modulus for cement used in oilfields [35]. We consider correlations between fracture energy and Young's modulus of three types: constant Γ_c, linear dependence of Γ_c on E_c, and quadratic dependence of Γ_c on E_c (Fig. 5). The three types assume $\Gamma_c = 20\ \text{J/m}^2$ at $E_c/E_f = 0.6$. Also included as dashed lines are the maximum energy release rates $G_{\max}$ for $p = 30$, 40, and 50 MPa. The failsafe condition $G_{\max} < \Gamma_c$ sets different requirements for cement, depending on the internal pressure and the type of $\Gamma_c - E_c$ relation. For example, for the cement to avoid tunneling crack under internal pressure $p = 40\,\text{MPa}$, the value of E_c/E_f

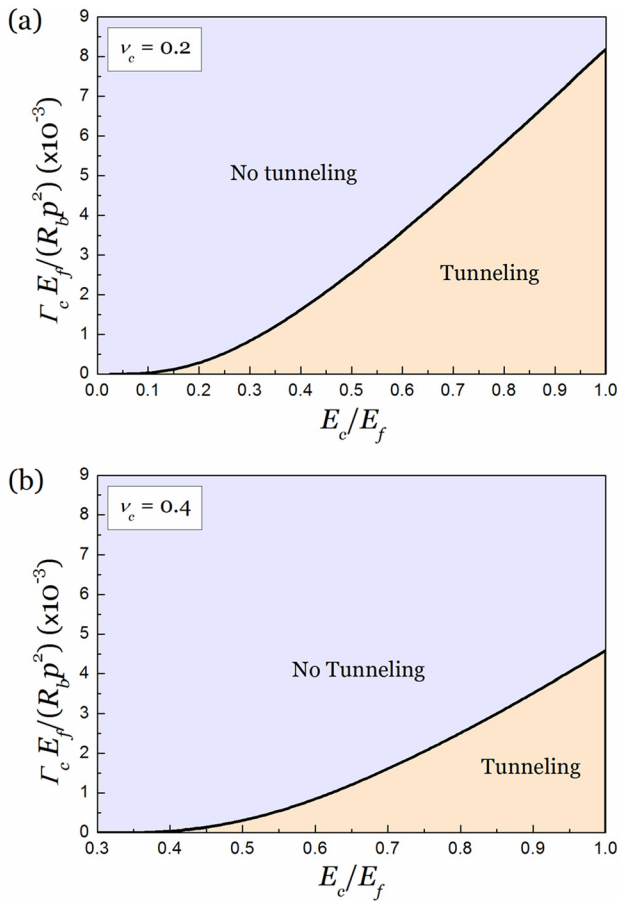

Fig. 4 Two regions exist on the plane with axes of the normalized Young's modulus and normalized fracture energy of the cement: (*a*) $\nu_c = 0.2$ and (*b*) $\nu_c = 0.4$

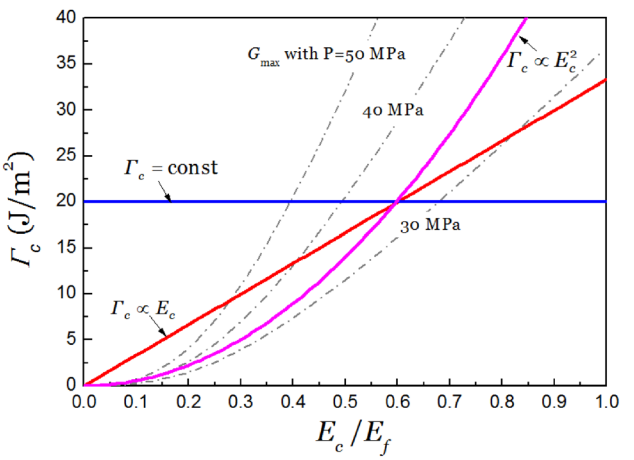

Fig. 5 The correlation between the fracture energy and elastic modulus of cement. The constant coefficient values are specified as $\nu_c = 0.2$, $E_f = 20\,\text{GPa}$, $\nu_f = 0.2$, $R_c = 80\,\text{mm}$, and $R_b = 100\,\text{mm}$.

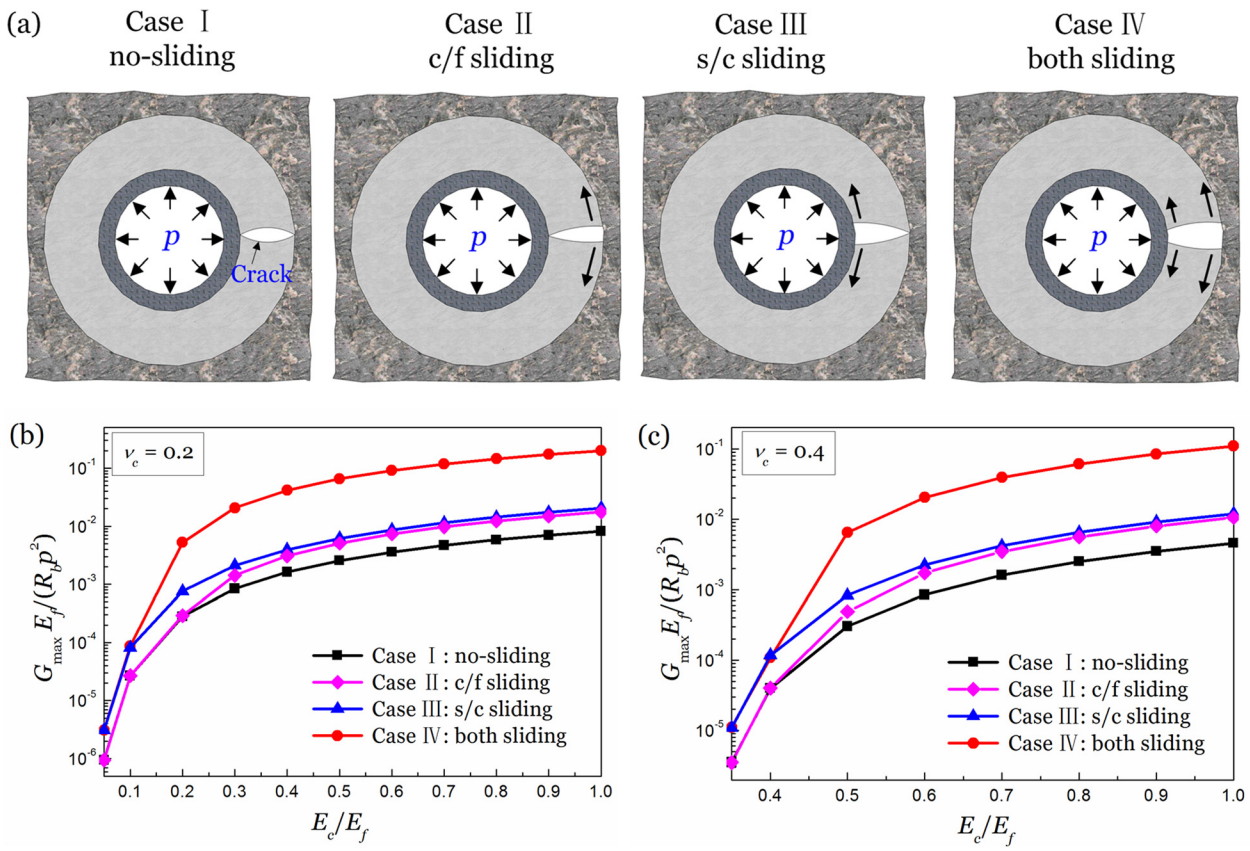

Fig. 6 The effect of interfacial sliding on energy release rate. (*a*) Four interfacial conditions. Each interface is either well-bonded or capable of frictionless sliding. The energy release rates as functions of Young's modulus of the cement for the four interfacial conditions for (*b*) $\nu_c = 0.2$ and (*c*) $\nu_c = 0.4$.

needs to be less than 0.5 for the type of constant Γ_c, 0.4 for the type of $\Gamma_c \sim E_c$, and 0.1 for the type of $\Gamma_c \sim E_c^2$.

Effects of Interfacial Sliding

The above results assume that the cement/casing and cement/formation interfaces are well bonded. In oilfields, the interfaces may not be bonded, and frictional forces can be small, e.g., due to the contamination of oil-based drilling fluid [36]. The stress analysis assumes that the deformation is axisymmetric, so that interfacial sliding plays no role in predicting the failure of cement. By contrast, the magnitude of interfacial sliding can significantly affect the energy release rate of a radial crack [30]. Here, we examine the effect of interfacial sliding on tunneling cracks. The lower the friction forces, the larger the crack-opening displacement $\delta(r)$. Consequently, the energy release rate of tunneling crack will increase with the decreasing frictional forces.

First, we consider four extreme interfacial conditions, with each interface being either well-bonded, or capable of frictionless sliding (Fig. 6). No-sliding and free-sliding conditions for both interfaces provide a lower and upper bound, respectively. The maximum energy release rates increase about two orders of magnitude between the two bounds. In other words, interfacial sliding can reduce the critical load for tunneling by an order of magnitude. In the other two cases, one interface is well-bonded and the other one is free-sliding. When the cement is compliant, the curve for the free-sliding cement/formation (*c*/*f*) interface nearly overlaps with the lower bound, whereas the curve for the free-sliding steel casing/cement (*s*/*c*) interface nearly overlaps with the upper bound. When the cement is stiff, these two curves are nearly indistinguishable and fall in between the upper and lower bounds. In oilfields, the ratio of modulus E_c/E_f is often low (~0.1), so that the frictional force in the steel casing/cement (*s*/*c*) interface is more effective to resist tunneling.

We also analyze cases with interfaces of finite friction coefficient μ (Fig. 7). In contrast to upper and lower bounds, the normalized energy release rates $G_{\max}E_f/(R_bp^2)$ for finite friction coefficients are no longer constant with respect to p. They decrease with increasing p, because the frictional forces in the interfaces, which resist the crack from opening, become significant for large p. When $p = 50$ MPa, the case with $\mu = 0.01$ is close to free-sliding condition (upper bound) while the case with $\mu = 0.5$ almost converges to the no-sliding case (lower bound). The friction coefficients for the former and latter cases are typical values for cement/casing interface with and without contamination of drilling mud. These results further demonstrate the importance of mud-removal on the crack-resistance of cement.

Conclusions

This work studies cracks tunneling in cement sheath. Tunnels will not form if the maximum energy release rate is less than the fracture energy of the cement. This failsafe condition requires no measurement of small cracks, but depends on material properties and operating conditions. Cement with lower Young's modulus and higher Poisson's ratio better resists tunneling cracks. The decrease of Young's modulus, however, often results in a decrease of fracture energy, which must be examined with care. Interfacial sliding can significantly reduce the critical load for tunneling crack.

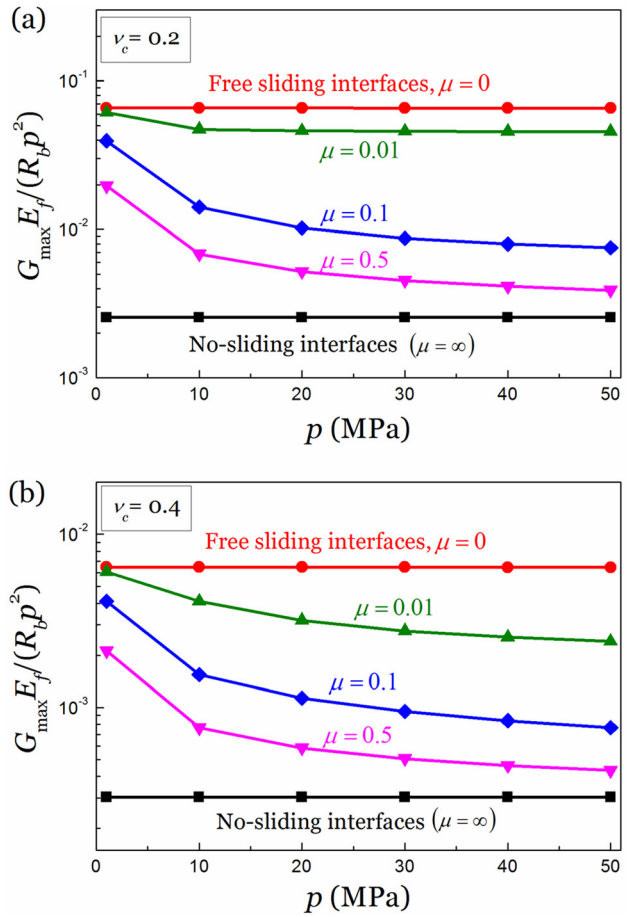

Fig. 7 The effect of friction on the energy release rate. The modulus ratio of cement $E_c/E_f = 0.5$. Poisson's ratios for the cement are chosen as: (*a*) $\nu_c = 0.2$ and (*b*) $\nu_c = 0.4$.

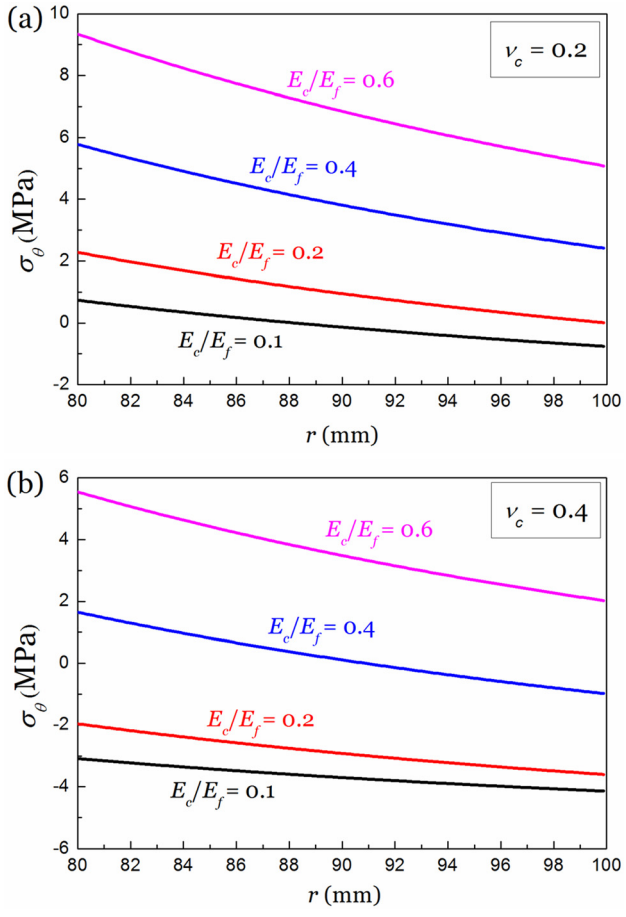

Fig. 8 The hoop stress, σ_θ, in the cement sheath when $p = 50$ MPa, $E_f = 20$ GPa, $\nu_f = 0.2$, $R_c = 80$ mm, $t_s = 10$ mm, and $R_b = 100$ mm: (*a*) $\nu_c = 0.2$ and (*b*) $\nu_c = 0.4$

Acknowledgment

The research work done at the Harvard was supported by MRSEC (DMR-14-20570) and by Schlumberger. Wang was supported by the China Scholarship Council as a visiting scholar for 2 years at the Harvard University.

Appendix A: Stresses in Cement Sheath Prior to Cracking

The stress state prior to cracking can be obtained analytically as the solution to the Lame´ problem in the linear theory of elasticity. We assume that steel casing, cement, and formation are three coaxial cylinders with a different Young's modulus and Poisson's ratio. Under the axisymmetric condition, the strains in radial and circumferential directions, ε_r and ε_θ, are given by

$$\varepsilon_r = \frac{du}{dr}, \quad \varepsilon_\theta = \frac{u}{r} \tag{A1}$$

where u is the displacement in radial direction. The strains relate to the stresses by Hooke's law

$$\begin{aligned} \varepsilon_r &= \frac{1-\nu^2}{E}\left(\sigma_r - \frac{\nu}{1-\nu}\sigma_\theta\right) \\ \varepsilon_\theta &= \frac{1-\nu^2}{E}\left(\sigma_\theta - \frac{\nu}{1-\nu}\sigma_r\right) \end{aligned} \tag{A2}$$

where σ_r and σ_θ are the stresses in radial and circumferential directions. The balance of forces requires that

$$\frac{d\sigma_r}{dr} + \frac{\sigma_r - \sigma_\theta}{r} = 0 \tag{A3}$$

Solving Eqs. (A1)–(A3) gives analytical solutions for the displacement fields in each cylindrical layer

$$u_i = a_i r + \frac{b_i}{r} \quad \text{where } i = s, c, \text{ and } f \tag{A4}$$

where subscripts s, c, and f refer to steel casing, cement, and formation, respectively. The values of a_i and b_i can be determined with the loading boundary condition in the inner surface of casing, zero displacement condition with r reaching infinity and continuous interfacial conditions

Figure 8 plots the hoop stress inside the cement sheath with low and high Poisson's ratio, respectively. The hoop stress decreases from cement/casing to cement/formation interface. Hoop stress decreases with increasing Poisson's ratio and decreasing Young's modulus of cement. In cases $E_c/E_f = 0.2$ or 0.1 and $\nu_c = 0.4$, the hoop stresses are compressive inside the cement sheath.

Appendix B: Crack-Opening Displacement $\delta(r)$

We use a commercial finite-element software ABAQUS to simulate the crack opening inside the cement sheath. We simulate half of the cross section of the wellbore with a symmetric boundary

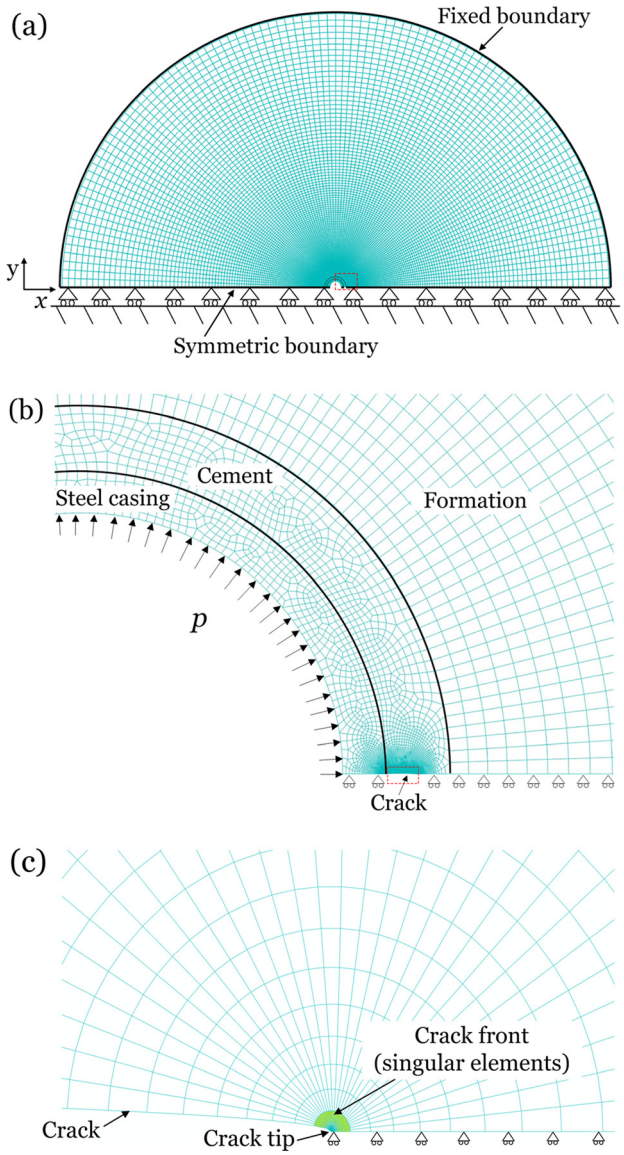

Fig. 9 Finite-element model for cement sheath: (*a*) meshed symmetric model, (*b*) refined mesh near the crack, and (*c*) characteristic of the contour integrals around the crack tip

condition (Fig. 9). A crack starting from the cement/casing interface is placed along the symmetric axis. A pressure p is applied on the inner surface of the steel casing. The domain size of formation is chosen to be large enough, i.e., 100 times as that of the borehole, to ensure it has insignificant effect on the simulation results.

Eight-node biquadratic plane strain quadrilateral elements are adopted for all the three layers of steel casing, cement sheath, and formation except the crack tip region, where singular elements are constructed (Fig. 9(*c*)). To obtain accurate opening profile, sufficiently refined meshes are applied in the vicinity of the crack.

References

[1] Gandossi, L., 2013, *An Overview of Hydraulic Fracturing and Other Formation Stimulation Technologies for Shale Gas Production*, Publications Office of the European Union, Luxembourg.

[2] Allouche, E. N., Ariaratnam, S. T., and Lueke, J. S., 2000, "Horizontal Directional Drilling: Profile of an Emerging Industry," J. Constr. Eng. Manage., **126**(1), pp. 68–76.

[3] Beckwith, R., 2010, "Hydraulic Fracturing: The Fuss, The Facts, The Future," J. Pet. Technol., **62**(12), pp. 34–40.

[4] Montgomery, C. T., and Smith, M. B., 2010, "Hydraulic Fracturing: History of an Enduring Technology," J. Pet. Technol., **62**(12), pp. 26–40.

[5] Rahman, M. M., and Rahman, M. K., 2010, "A Review of Hydraulic Fracture Models and Development of an Improved Pseudo-3D Model for Stimulating Tight Oil/Gas Sand," Energy Sources, Part A, **32**(15), pp. 1416–1436.

[6] Wong, S.-W., Geilikman, M., and Xu, G., 2013, "Interaction of Multiple Hydraulic Fractures in Horizontal Wells," SPE Unconventional Gas Conference and Exhibition, Muscat, Oman, Society of Petroleum Engineers, Paper No. SPE-163982-MS, pp. 335–344.

[7] Bažant, Z. P., Salviato, M., Chau, V. T., Viswanathan, H., and Zubelewicz, A., 2014, "Why Fracking Works," ASME J. Appl. Mech., **81**(10), p. 101010.

[8] Wicks, N., Wardle, B. L., and Pafitis, D., 2008, "Horizontal Cylinder-in-Cylinder Buckling Under Compression and Torsion: Review and Application to Composite Drill Pipe," Int. J. Mech. Sci., **50**(3), pp. 538–549.

[9] Cawiezel, K. E., and Gupta, D. V. S., 2010, "Successful Optimization of Viscoelastic Foamed Fracturing Fluids With Ultralightweight Proppants for Ultralow-Permeability Reservoirs," SPE Prod. Oper., **25**(1), pp. 80–88.

[10] Gaurav, A., Dao, E. K., and Mohanty, K. K., 2012, "Evaluation of Ultra-Light-Weight Proppants for Shale Fracturing," J. Pet. Sci. Eng., **92–93**, pp. 82–88.

[11] Musso, S., Robisson, A., Maheshwar, S., and Ulm, F.-J., 2014, "Stimuli-Responsive Cement-Reinforced Rubber," ACS Appl. Mater. Interfaces, **6**(9), pp. 6962–6968.

[12] Cai, S., Lou, Y., Ganguly, P., Robisson, A., and Suo, Z., 2010, "Force Generated by a Swelling Elastomer Subject to Constraint," J. Appl. Phys., **107**(10), p. 103535.

[13] Liu, Q., Robisson, A., Lou, Y., and Suo, Z., 2013, "Kinetics of Swelling Under Constraint," J. Appl. Phys., **114**(6), p. 064901.

[14] Liu, Q., Wang, Z., Lou, Y., and Suo, Z., 2014, "Elastic Leak of a Seal," Extreme Mech. Lett., **1**, pp. 54–61.

[15] Wang, Z., Liu, Q., Lou, Y., Jin, H., and Suo, Z., 2015, "Elastic Leak for a Better Seal," ASME J. Appl. Mech., **82**(8), p. 081010.

[16] Lou, Y., and Chester, S., 2014, "Kinetics of Swellable Packers Under Downhole Conditions," ASME Int. J. Appl. Mech., **6**(6), p. 1450073.

[17] Aviles, I., Marya, M., Reyes Hernandez, T., Dunne, T., Dardis, M., and Baihly, J. D., 2013, "Application and Benefits of Degradable Technology in Open-Hole Fracturing," SPE Annual Technical Conference and Exhibition, New Orleans, LA, Sept. 30–Oct. 2, Society of Petroleum Engineers, Paper No. SPE-166528-MS.

[18] Aviles, I., Dardis, M., and Jacob, G., 2015, "Degradable Alternative to Risky Mill-Out Operations in Plug and Perf," SPE/ICoTA Coiled Tubing & Well Intervention Conference and Exhibition, The Woodlands, TX, Mar. 24–25, Society of Petroleum Engineers, Paper No. SPE-173695-MS.

[19] Nelson, E. B., 1990, *Well Cementing*, Elsevier, New York.

[20] Goodwin, K. J., and Crook, R. J., 1992, "Cement Sheath Stress Failure," SPE Drill. Eng., **7**(4), pp. 291–296.

[21] Jackson, P. B., and Murphey, C. E., 1993, "Effect of Casing Pressure on Gas Flow Through a Sheath of Set Cement," SPE/IADC Drilling Conference, Amsterdam, The Netherlands, Feb. 2–5, Society of Petroleum Engineers, Paper No. SPE-25698-MS.

[22] Thiercelin, M. J., Dargaud, B., Baret, J. F., and Rodriguez, W. J., 1997, "Cement Design Based on Cement Mechanical Response," SPE Annual Technical Conference and Exhibition, San Antonio, TX, Oct. 5–8, Society of Petroleum Engineers, Paper No. SPE-38598-MS.

[23] Bourgoyne, A., Scott, S., and Manowski, W. A., 2000, "Review of Sustained Casing Pressure Occurring on the OCS," Report No. 14-35-001-30749.

[24] Tellisi, M., Ravi, K., and Pattillo, P., 2005, "Characterizing Cement Sheath Properties for Zonal Isolation," 18th World Petroleum Congress, Johannesburg, South Africa, Paper No. WPC-18-0865, pp. 1–5.

[25] Bosma, M., Ravi, K., van Driel, W., and Schreppers, G. J., 1999, "Design Approach to Sealant Selection for the Life of the Well," SPE Annual Technical Conference and Exhibition, Houston, TX, Oct. 3–6, Society of Petroleum Engineers, Paper No. SPE-56536-MS.

[26] Stiles, D., and Hollies, D., 2002, "Implementation of Advanced Cementing Techniques to Improve Long Term Zonal Isolation in Steam Assisted Gravity Drainage Wells," SPE International Thermal Operations and Heavy Oil Symposium and International Horizontal Well Technology Conference, Calgary, Canada, Nov. 4–7, Society of Petroleum Engineers, Paper No. SPE-78950-MS.

[27] Tahmourpour, F., and Griffith, J., 2007, "Use of Finite Element Analysis to Engineer the Cement Sheath for Production Operations," J. Can. Pet. Technol., **46**(5), pp. 10–13.

[28] DeBruijn, G. G., Garnier, A., Brignoli, R., Bexte, D. C., and Reinheimer, D., 2009, "Flexible Cement Improves Wellbore Integrity in SAGD Wells," SPE/IADC Drilling Conference and Exhibition, Amsterdam, The Netherlands, Mar. 17–19, Society of Petroleum Engineers, Paper No. SPE-119960-MS.

[29] Garnier, A., Saint-Marc, J., Bois, A.-P., and Kermanac'h, Y., 2010, "An Innovative Methodology for Designing Cement-Sheath Integrity Exposed to Steam Stimulation," SPE Drill. Completions, **25**(1), pp. 58–69.

[30] Ulm, F., Abuhaikal, M., Petersen, T., and Pellenq, R., 2014, "Poro-Chemo-Fracture-Mechanics… Bottom-Up: Application to Risk of Fracture Design of Oil and Gas Cement Sheath at Early Ages," *Computational Modelling of Concrete Structures*, Vol. 1, CRC Press, St. Anton am Alberg, Austria, p. 61.

[31] Carter, L. G., Slagle, K. A., and Smith, D. K., 1968, "Stress Capabilities Improved by Resilient Cement," Drilling and Production Practice, American Petroleum Institute, New York, Paper No. API-68-029, pp. 29–37.

[32] Boukhelifa, L., Moroni, N., James, S., Le Roy-Delage, S., Thiercelin, M. J., and Lemaire, G., 2005, "Evaluation of Cement Systems for Oil and Gas Well Zonal

Isolation in a Full-Scale Annular Geometry," SPE Drill. Completions, **20**(1), pp. 44–53.
[33] Ho, S., and Suo, Z., 1992, "Microcracks Tunneling in Brittle Matrix Composites Driven by Thermal Expansion Mismatch," Acta Metall. Mater., **40**(7), pp. 1685–1690.
[34] Hutchinson, J. W., and Suo, Z., 1992, "Mixed Mode Cracking in Layered Materials," Adv. Appl. Mech., **29**(63), p. 191.
[35] Ulm, F.-J., and James, S., 2011, "The Scratch Test for Strength and Fracture Toughness Determination of Oil Well Cements Cured at High Temperature and Pressure," Cem. Concr. Res., **41**(9), pp. 942–946.
[36] Biezen, E., van der Werff, N., and Ravi, K., "Experimental and Numerical Study of Drilling Fluid Removal From a Horizontal Wellbore," SPE Annual Technical Conference and Exhibition, Dallas, TX, Oct. 1–4, Society of Petroleum Engineers, Paper No. SPE-62887-MS.